Rh-TPPTS Intercalated Layered Double Hydroxides as Hydroformylation Catalyst

Min Wei, Xian Zhang, David G. Evans, and Xue Duan
State Key Laboratory of Chemical Resource Engineering, Beijing University of Chemical Technology, Beijing 100029, P.R. China

Xianjun Li and Hua Chen
Dept. of Chemistry, Sichuan University, Chengdu 610064, P.R. China

DOI 10.1002/aic.11324
Published online September 28, 2007 in Wiley InterScience (www.interscience.wiley.com).

Trans-RhCl(CO)(TPPTS)$_2$ [TPPTS, trisodium salt of tri-(m-sulfophenyl)-phosphine] and TPPTS ligands have been cointercalated into zinc–aluminum-layered double hydroxides (ZnAl-LDHs) by in situ complexation, and the catalytic performances of the resulting materials for 1-hexene hydroformylation have been investigated. The intercalated materials were characterized by means of XRD, FTIR, ICP, and ^{31}P MAS NMR. The rhodium complex and TPPTS ligands coexist in the interlayer galleries of LDH (denoted as RhP$_2$-P-Zn$_n$Al-LDH, where n denotes as the molar ratio Zn/Al), with an interlayer spacing of ca. 1.58 nm. Compared with the catalytic properties of the corresponding water-oil biphasic catalyst under similar reaction conditions, RhP$_2$-P-Zn$_3$Al-LDH showed better reusability and activity. Furthermore, compared with a related material prepared by ion exchange, the RhP$_2$-P-Zn$_3$Al-LDH showed better activity and selectivity towards aldehyde. The influence of the Zn/Al molar ratio in RhP$_2$-P-Zn$_n$Al-LDH has also been studied, and it was found that higher selectivity to aldehydes and lower activity were obtained with increasing Zn/Al molar ratio. *AIChE J,* 53: 2916–2924, 2007
Keywords: trans-RhCl(CO)(TPPTS)$_2$, layered double hydroxide, intercalation, hydroformylation, in situ complexation

Introduction

Hydroformylation, the addition of synthesis gas (CO and H_2) to alkenes, is one of the most important syngas-related reactions.[1] The hydroformylation reaction was first discovered using a heterogeneous Fischer-Tropsch catalyst.[2] As one of the mildest and cleanest methods to produce aldehydes, it is widely applied in the petrochemical industry. All current commercial processes are based on homogeneous catalysts, mostly using rhodium. Over the past few decades, however, development and application of immobilized homogeneous catalysts have been attracting widespread interest,[3–5] since such catalysts can combine the high activity and selectivity of homogeneous catalysts with the long lifetime and ease of separation of heterogeneous catalysts.[6] A large number of papers and patents concerning alkene hydroformylation catalyzed by rhodium or other noble metal complexes supported on silica or other oxide supports have been published[7,8] and, moreover, the encapsulation of such complexes in microporous and mesoporous supports,[9] construction through a "ship-in-the-bottle" process in zeolites,[10] and entrapment in sol-gel structures[11] or "host-guest" structures[12] have also

Correspondence concerning this article should be addressed to X. Duan at duanx@mail.buct.edu.cn.

been studied. It has been reported that some of these catalysts are highly effective hydroformylation catalysts.

Layered double hydroxides (LDHs) are a class of synthetic anionic clays whose structure is based on brucite ($Mg(OH)_2$)-like layers in which some of the divalent cations have been replaced by trivalent ions giving positively-charged sheets.[13–15] This charge is balanced by intercalation of anions in the hydrated interlayer regions. LDHs can be represented by the general formula $[M^{II}_{1-x}M^{III}_x(OH)_2]^{x+}(A^{n-})_{x/n}.yH_2O$. The identities of the di- and trivalent cations (M^{II} and M^{III}, respectively) and the interlayer anion (A^{n-}) together with the value of the stoichiometric coefficient (x) may be varied over a wide range, giving rise to a large class of isostructural materials. These layered solids have received considerable attention because of their many practical applications, including as nanocomposite materials,[16] functional materials,[17] and catalysts.[13,18,19] One attractive feature of such materials is that they serve as a template for the formation of supramolecular structures,[20] and many new species can be assembled by reaction of guest compounds in the LDH matrices.[13,17] There have been some reports of intercalation of transition metal complexes in LDHs giving materials with expanded interlayer spacing, which have shown good catalytic activity. Examples include dioxomolybdenum (VI) complexes,[21] cobalt (II) macrocylic complexes,[22] and manganese (III) complexes of Schiff base ligands.[23] In other cases, catalytic activity was observed with no expansion of interlayer spacing, suggesting that the catalytically active anion was adsorbed on edge sites as in the case of WO_4^{2-}[18] or $PdCl_4^{2-}$.[24]

In our previous work, the intercalation of *trans*-RhCl(CO)$(TPPTS)_2$ [TPPTS: trisodium salt of tri-(*m*-sulfophenyl)-phosphine, $P(m\text{-}C_6H_4SO_3Na)_3$] into zinc–aluminum-layered double hydroxides (ZnAl-LDHs) was performed by the method of ion-exchange, and the resulting composite material was structurally characterized.[25] To the best of our knowledge, except for this work,[25] there has been only one other reported attempt to immobilize a water soluble phosphine transition metal complex on an LDH viz. reaction of *cis*-$Pd(TPPTS)_2Cl_2$ and MgAl-Cl-LDH afforded a material with unchanged interlayer spacing, indicating that the palladium complex was immobilized on the edge of the crystallites.[26] At the start of the work reported here, we studied the catalytic performance of *trans*-RhCl(CO)$(TPPTS)_2$ intercalated LDH in hydroformylation, but found that its catalytic properties were somewhat disappointing. As a result, the aim of this work is to prepare heterogenized rhodium complex catalysts based on composites of *trans*-RhCl(CO)$(TPPTS)_2$ and intercalated ZnAl-LDHs with improved catalytic performance in hydroformylation. In particular, *trans*-RhCl(CO)$(TPPTS)_2$ has been intercalated into ZnAl-LDHs in the presence of free TPPTS as the cointercalated component (to give materials denoted as RhP_2-P-Zn_nAl-LDH, n = 2, 3, and 4) by a method of in situ complexation. The catalytic performance of the new cointercalated material was compared with that of the corresponding biphasic catalyst system under similar reaction conditions, in which *trans*-RhCl(CO)$(TPPTS)_2$ and TPPTS were untethered, and *trans*-RhCl(CO)$(TPPTS)_2$ intercalated ZnAl-LDH prepared via ion-exchange. Therefore, this work provides a new Rh-phosphine complex-inorganic layered material with prospective application.

Experimental Section

Catalyst preparation

Synthesis of Trans-RhCl(CO)$(TPPTS)_2$. TPPTS was prepared according to a standard literature procedure.[27] *Trans*-RhCl(CO)$(TPPTS)_2$ was prepared as a pale yellow powder according to the procedure described in a Chinese patent[25,28] and characterized by microanalysis; found (calculated) wt.%: P 4.67 (4.76), S 15.04 (14.74), Rh 7.58 (7.91); P/Rh 1.9 (2.0), S/P 2.9 (3.0).

Preparation of Trans-RhCl(CO)$(TPPTS)_2$ Intercalated ZnAl-LDHs. Ion-Exchange Method. The precursor $[Zn_3Al(OH)_8](NO_3)\cdot 4H_2O$, (denoted as NO_3-Zn_3Al-LDH) was synthesized by a literature procedure.[29] Intercalation of *trans*-RhCl(CO) $(TPPTS)_2$ into LDH was carried out by the method of ion-exchange as reported previously.[25] The sample is denoted as RhP_2-Zn_3Al-LDH.

In Situ Complexation Method. A TPPTS preintercalated ZnAl-LDH precursor (denoted as TPPTS-Zn_3Al-LDH) was first prepared by the method of ion exchange, in which a mixture of the precursor NO_3-Zn_3Al-LDH (5.00 g, 1.80 mmol) and an aqueous solution of TPPTS (1.02 g, 1.80 mmol) was heated at 80°C under a nitrogen atmosphere for 72 h. A solution of $RhCl_3\cdot 3H_2O$ (0.02 g, 6.90×10^{-2} mmol) in pure ethanol (10 ml) was held at 78°C under a carbon monoxide atmosphere for 50 min. A suspension of TPPTS-Zn_3Al-LDH (1.00 g, 0.42 mmol) in distilled, deionized water (5 ml) was then added dropwise quickly. The mixture was held at 78°C for 40 min, after which pure ethanol was added to cool the mixture. The resulting precipitate was separated, washed with pure ethanol, and dried in vacuo at 60°C. The product is denoted as RhP_2-P-Zn_3Al-LDH. Other intercalates with different Zn/Al molar ratios were obtained by the same method (denoted as RhP_2-P-Zn_2Al-LDH and RhP_2-P-Zn_4Al-LDH, respectively). It was found that the color of the composite material changed from white in the case of the precursor (TPPTS-Zn_nAl-LDH, n = 2, 3, 4) to pale yellow in the cases of the resulting RhP_2-P-Zn_nAl-LDH (n = 2, 3, 4), indicating the formation of the Rh-phosphine complex via in situ complexation.

Characterization

XRD measurements were performed on a Rigaku XRD-6000 diffractometer, using Cu K_α radiation (λ = 0.154 nm) at 40 kV, 30 mA, a scanning rate of 0.02 °/s, in the 2θ range 3° to 70°.

FTIR spectra were recorded using a Bruker Vector22 spectrophotometer in the range 4000–400 cm^{-1} with 2 cm^{-1} resolution. The standard KBr disk method (1 mg of sample in 100 mg of KBr) was used.

^{31}P MAS NMR spectra were recorded on a Bruker AV300 spectrometer operating at a frequency of 121.497 MHz for ^{31}P at a spinning rate of −8000 Hz with a 10 s pulse delay.

Elemental analysis was performed by ICP emission spectroscopy on a Shimadzu ICPS-7500 instrument using solutions prepared by dissolving the samples in dilute HCl.

Thermogravimetric analysis and differential thermal analysis (TG/DTA) were measured in air using a PCT-1A thermal analysis system with a heating rate of 10°C/min.

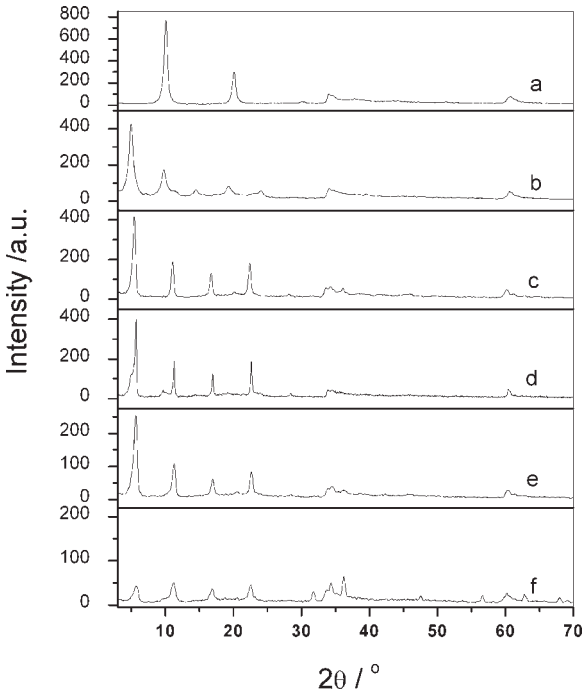

Figure 1. Powder XRD patterns of (a) NO_3-Zn_3Al-LDH, (b) RhP_2-Zn_3Al-LDH, (c) TPPTS-Zn_3Al-LDH, (d) RhP_2-P-Zn_2Al-LDH, (e) RhP_2-P-Zn_3Al-LDH, and (f) RhP_2-P-Zn_4Al-LDH.

Catalytic testing

Hydroformylation of 1-hexene was conducted under 1.6 MPa of an equimolar CO and H_2 mixture at 100°C in a stainless steel autoclave with a magnetic stirrer. The rhodium-containing catalyst (Rh/1-hexene = 4.0×10^{-4}), 1-hexene (1.5 ml), toluene (3 ml), and triethylamine (0.05 ml) were first transferred to the autoclave. The reaction system was purged with the CO + H_2 mixture and subsequently charged to the working pressure. When a reaction cycle was completed, the reactor was allowed to cool to room temperature and depressurized. The solid catalyst was reclaimed in a sealed tube by centrifugal separation for 3 min and the cycle repeated. The products of hydroformylation were analyzed by GC-MS using a Shimadzu 2010 instrument.

Results and Discussion

Structure of the catalysts and their precursors

The powder XRD patterns of NO_3-Zn_3Al-LDH and the intercalated materials produced by the method of ion-exchange and in situ complexation with different Zn/Al molar ratios are shown in Figure 1, The basal spacing and lattice parameters are listed in Table 1. In each case, the reflections can be indexed to a hexagonal lattice with *R-3m* rhombohedral symmetry, commonly used[30,31] for the description of LDH structures. However, as is often the case,[32] several of the (*hkl*) reflections disappear or broaden in the samples prepared by the method of both ion-exchange and in situ complexation. The NO_3-Zn_3Al-LDH precursor has an XRD pattern (Figure 1a) similar to those reported previously,[33] with a basal spacing (d_{003}) of 0.88 nm (Table 1). After reaction with *trans*-RhCl(CO)$(TPPTS)_2$ by the method of ion exchange, the basal reflection in the XRD pattern of RhP_2-Zn_3Al-LDH (Figure 1b) was observed at 4.96°, corresponding to an expanded basal spacing of 1.78 nm (Table 1). The XRD pattern of the precursor TPPTS-Zn_3Al-LDH (Figure 1c) indicates that the material has a basal spacing of 1.63 nm. After the in situ complexation reaction however, the 003 reflections of RhP_2-P-Zn_2Al-LDH, RhP_2-P-Zn_3Al-LDH, and RhP_2-P-Zn_4Al-LDH appear at 5.60, 5.64, and 5.66°, with the corresponding basal spacings (d_{003}) of 1.57, 1.58 and 1.56 nm, respectively, representing a contraction of the interlayer distance compared with the precursor. This is rather interesting and is consistent with the occurrence of a chemical reaction and the reorientation of the interlayer guests. A significant decrease in the reflection intensity as well as increase in the peak width at half height were observed as the Zn/Al ratio in RhP_2-P-Zn_nAl-LDH increased from n = 1.9 to 2.6 to 3.9 (Figures 1d–f). A small amount of an impurity phase was also found in RhP_2-P-Zn_4Al-LDH. The basal spacing of the material prepared by ion-exchange is much larger than that of the materials prepared by in situ complexation (1.78 and 1.56–1.58 nm, respectively), which suggests that different spatial orientation of the interlayer anions are involved. This will be further discussed in the ^{31}P MAS NMR section below.

The FTIR spectra of TPPTS, *trans*-RhCl(CO)$(TPPTS)_2$, and their intercalates in the LDHs are shown in Figure 2. The spectra of TPPTS and *trans*-RhCl(CO)$(TPPTS)_2$ (Figures 2a and b) are similar to those reported in the literature.[34] In the case of the intercalated materials, the broad bands at around 3443 cm^{-1} (Figures 2c–g) can be attributed to O—H stretching vibrations of surface and interlayer water molecules,[13] which are found at lower frequency in LDHs compared with the O—H stretching vibrations of free water at 3600 cm^{-1}.[35] This suggests the presence of hydrogen bonding between interlayer water and the guest anions as well as the layer hydroxide groups. The bands at 1196, 1040, and 628 cm^{-1} of TPPTS (Figure 2a) and *trans*-RhCl(CO)$(TPPTS)_2$ (Figure 2b) can be attributed to the stretching

Table 1. XRD Data and Lattice Parameters of NO_3-Zn_3Al-LDH and the Intercalated Materials

	NO_3-Zn_3 Al-LDH	RhP_2-Zn_3 Al-LDH	TPPTS-Zn_3 Al-LDH	RhP_2-P-Zn_2 Al-LDH	RhP_2-P-Zn_3 Al-LDH	RhP_2-P-Zn_4 Al-LDH
d_{003}/nm	0.88	1.78	1.63	1.57	1.58	1.56
d_{006}/nm	0.44	0.90	0.80	0.78	0.79	0.79
d_{009}/nm	0.26	0.46	0.53	0.52	0.52	0.53
d_{110}/nm	0.15	0.15	0.15	0.15	0.15	0.15
Lattice parameter *a*/nm	0.30	0.30	0.30	0.30	0.30	0.30
Lattice parameter *c*/nm	2.64	5.34	4.89	4.71	4.74	4.68

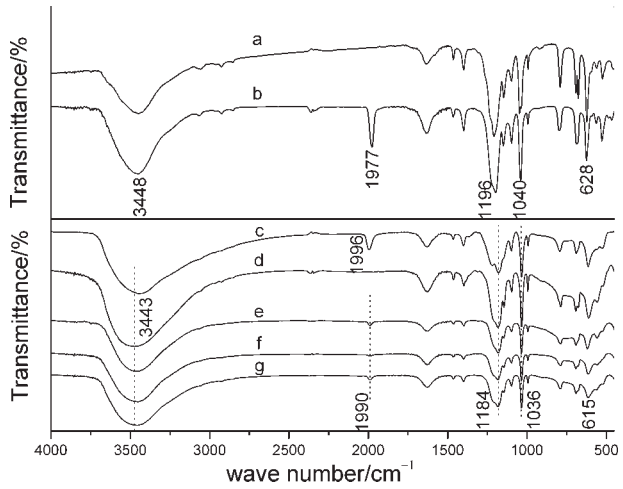

Figure 2. FTIR spectra of (a) TPPTS, (b) *trans*-RhCl(CO)(TPPTS)$_2$, (c) RhP$_2$-Zn$_3$Al-LDH, (d) TPPTS-Zn$_3$Al-LDH, (e) RhP$_2$-P-Zn$_2$Al-LDH, (f) RhP$_2$-P-Zn$_3$Al-LDH, and (g) RhP$_2$-P-Zn$_4$Al-LDH.

vibrations ν_{oso}, ν_{so}, and ν'_{so}, respectively. After intercalation into the LDH host, these three bands move to lower frequency, being observed at 1184, 1036, and 615 cm^{-1} (Figures 2c–g), respectively. It is known that the coordination of the oxygen atom in the sulfonate group decreases the force constant in the S—O bond and accordingly results in a shift of the S—O vibration band to lower frequency[36]; this has been previously reported in the FTIR spectra of the intercalates of naphthalene-2,6-disulfonate[37,38] and 9,10-anthraquinone-1,2-dihydroxy-3-sulfonate (Alizarin red S anion) in LDHs.[39] Therefore, it can be concluded that the observed shift of these bands results from the interaction between the oxygen atom in the sulfonate group of the interlayer *trans*-RhCl(CO)(TPPTS)$_2$ or TPPTS and the host lattice. The ν_{CO} stretching vibration of the pristine *trans*-RhCl(CO)(TPPTS)$_2$ (Figure 2b) appears at 1977 cm^{-1}, while this band in RhP$_2$-Zn$_3$Al-LDH (Figure 2c) and RhP$_2$-Zn$_n$Al-LDH (Figures 2e–g) was observed at 1996 and 1990 cm^{-1}, respectively, representing shifts of 19 and 13 cm^{-1} to higher frequency compared with the free complex. The frequencies of all the other main absorption bands of RhP$_2$-Zn$_3$Al-LDH (Figure 2c) and RhP$_2$-P-Zn$_n$Al-LDH (Figures 2e–g), such as the bands centered at 1466 and 1400 cm^{-1} corresponding to phenyl ring vibrations and at 797 and 690 cm^{-1} attributed to C—H out-of-plane bending vibrations of phenyl rings, closely resemble those in the spectra of both free *trans*-RhCl(CO)(TPPTS)$_2$ (Figure 2b) and TPPTS (Figure 2a). These data confirm that *trans*-RhCl(CO)(TPPTS)$_2$ can be intercalated between the layers of LDHs by both ion-exchange and in situ complexation methods.

Figure 3 shows the ^{31}P MAS NMR spectra of pristine TPPTS (Figure 3a), *trans*-RhCl(CO)(TPPTS)$_2$ (Figure 3b), the ion-exchange product RhP$_2$-Zn$_3$Al-LDH (Figure 3c), the TPPTS intercalated LDH precursor TPPTS-Zn$_3$Al-LDH (Figure 3d), and the in situ complexation product RhP$_2$-P-Zn$_3$Al-LDH (Figure 3e). The spectra of the pristine TPPTS (Figure 3a) and *trans*-RhCl(CO)(TPPTS)$_2$ (Figure 3b) show resonances at –5.5 and 32.3 ppm, respectively, which compare well with the literature values of –5.2 ppm for TPPTS and 32.5 ppm for *trans*-RhCl(CO)(TPPTS)$_2$.[1,40] In the case of RhP$_2$-Zn$_3$Al-LDH obtained by ion-exchange (Figure 3c), the broad signal at about 30.5 ppm can be assigned to the *trans*-RhCl(CO)(TPPTS)$_2$ in the interlayer galleries of the LDHs. Comparison of Figures 3a and d indicates that the ^{31}P resonance shifts from –5.5 ppm for free TPPTS (Figure 3a) to –20.2 ppm for its intercalated composite with LDH (Figure 3d). To determine whether this remarkable shift is indicative of decomposition of TPPTS during the intercalation process, a sample of TPPTS-Zn$_3$Al-LDH was subsequently stirred with an aqueous solution of sodium carbonate heated at 40°C under a nitrogen atmosphere for 24 h. Since carbonate anions have a very strong affinity for LDH layers and would be expected to displace the interlayer guest anions in TPPTS-Zn$_3$Al-LDH. After filtration of the mixture, the ^{31}P NMR spectrum of the filtrate showed an intense peak at –5.9 ppm, characteristic of TPPTS, together with a weak peak at 34.0 ppm, which is indicative of a small amount of TPPTS oxide, with no peak in the region around –20 ppm. Since the TPPTS was recovered essentially unchanged, the large difference in TPPTS chemical shift before and after intercalation is therefore a result of the host-guest interactions in the intercalate, rather than decomposition. The additional weak resonance at –7.2 ppm in Figure 3d may be attributed to a small amount of TPPTS adsorbed on the surface of LDH. As for the intercalated material RhP$_2$-P-Zn$_3$Al-LDH obtained by in situ complexation (Figure 3e), in addition to the two resonances at –20.6 and –7.2 ppm corresponding to intercalated and surface adsorbed TPPTS, respectively, another resonance was observed at 24.0 ppm, which can be assigned to the chemical shift of *trans*-RhCl(CO)(TPPTS)$_2$. This indicates that *trans*-RhCl(CO)(TPPTS)$_2$ is formed in the interlayer gallery of the precursor LDH (TPPTS-Zn$_3$Al-LDH) via in situ complexation, resulting in cointercalation of residual TPPTS and the rhodium complex. The difference between the ^{31}P chemical shifts of the in situ complexation product (24.0 ppm) and the ion-exchange product (30.5 ppm) is indicative of different

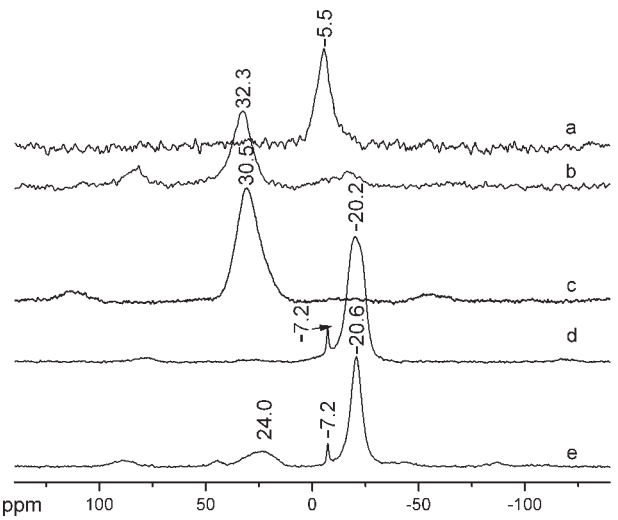

Figure 3. ^{31}P MAS NMR spectra of (a) TPPTS, (b) *trans*-RhCl(CO)(TPPTS)$_2$, (c) RhP$_2$-Zn$_3$Al-LDH, (d) TPPTS-Zn$_3$Al-LDH, and (e) RhP$_2$-P-Zn$_3$Al-LDH.

Table 2. Key Elemental Molar Ratios in *Trans*-RhCl(CO)(TPPTS)$_2$ and the Intercalated Materials

Sample	*Trans*-RhCl (CO)(TPPTS)$_2$	RhP_2-Zn_3 Al-LDH	TPPTS-Zn_3 Al-LDH	RhP_2-P-Zn_2 Al-LDH	RhP_2-P-Zn_3 Al-LDH	RhP_2-P-Zn_4 Al-LDH
Molar ratio Zn/Al	–	2.4	2.6	1.9	2.6	3.9
Molar ratio P/Rh	1.9	1.9	–	7.8	7.8	7.3
Rh (w/w) (%)	7.58	3.44	–	0.90	0.48	0.60

interlayer micro-environments of the phosphorus atom in the two complex-LDH composites, which can be related to the different spatial orientations of the interlayer anions. This is in consistent with the results of XRD, in which two different d_{003} values were obtained.

On the basis of elemental analysis data, key elemental molar ratios in *trans*-RhCl(CO)(TPPTS)$_2$ and the intercalated materials are listed in Table 2. It can be seen that the Zn/Al molar ratios of the intercalated materials are close to the value expected. The P/Rh molar ratio of RhP_2-Zn_3Al-LDH prepared by ion-exchange is the same as that of pristine *trans*-RhCl(CO)(TPPTS)$_2$, while this value in RhP_2-P-Zn_nAl-LDH prepared by in-situ complexation is much higher. This is in accordance with the cointercalation of TPPTS and *trans*-RhCl(CO)(TPPTS)$_2$, which has been demonstrated by ^{31}P MAS NMR. The P/Rh molar ratios in RhP_2-P-Zn_nAl-LDH are close to each other. The Rh loading in RhP_2-Zn_3Al-LDH is much higher than that in RhP_2-P-Zn_nAl-LDH, as a result of the presence of cointercalated TPPTS in the case of RhP_2-P-Zn_nAl-LDH. The difference in Rh content of the samples prepared by in situ complexation will be discussed in the next section.

The TG/DTA curves for RhP_2-P-Zn_3Al-LDH are shown in Figure 4 to study the thermal stability of the new catalyst. The thermal decomposition of RhP_2-P-Zn_3Al-LDH is characterized by four steps (Figure 4): the first loss event (50–150°C) corresponds to the dehydration of both the surface and interlayer water molecules with an endothermic peak at 100°C in the DTA curve; the second event (150–285°C) is due to the decomposition of the interlayer anions, and the corresponding endothermic peak is observed at 275°C; the third (285–460°C) is a consequence of dehydroxylation of the brucite-like layers and continued decomposition of interlayer anions; the fourth stage (460–580°C) is attributed to the further decomposition and combustion of interlayer materials with a strong exothermic peak at 540°C. The thermal decomposition process of RhP_2-P-Zn_3Al-LDH in this work is similar to that of *trans*-RhCl(CO)(TPPTS)$_2$ intercalated LDH materials in our previous report[25] except that the fourth loss event extends to a higher temperature (580°C). This might be related to the difference in both component and spatial orientations of the interlayer anions.

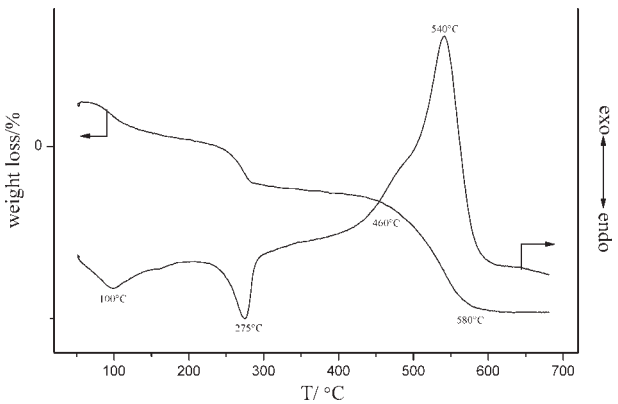

Figure 4. TG/DTA curves of RhP_2-P-Zn_3Al-LDH.

Catalytic performance in hydroformylation of 1-hexene and catalysis mechanism

Figure 5 depicts the catalytic results for four consecutive 10 h reaction cycles for the three catalyst systems studied,

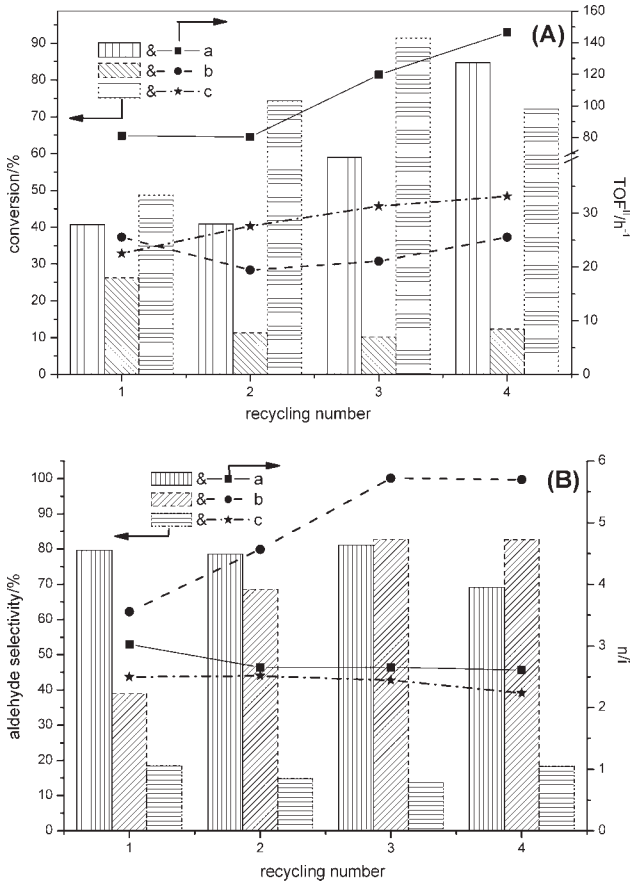

Figure 5. Activity (A) and selectivity (B) of (a) RhP_2-P-Zn_3Al-LDH,* (b) corresponding biphasic system (RhP_2 and TPPTS),† and (c) RhP_2-Zn_3Al-LDH catalyst* in hydroformylation‡ for 1-hexene.

*Rh/1-hexene = 4.0×10^{-4}; †TOF: mol aldehyde·mol^{-1} Rh·h^{-1}; ‡Reaction conditions: 1.5 ml of 1-hexene, 1.6 MPa, 100°C, H_2/CO = 1, 10 h per cycle.

viz. the system catalyzed by RhP_2-P-Zn_3Al-LDH prepared by in situ complexation, the corresponding water-oil biphasic catalytic system, and the one catalyzed by RhP_2-Zn_3Al-LDH prepared by the ion-exchange method. The three catalyst systems were studied under similar reaction conditions, such as temperature, pressure, solvent, stirring speed, and so on, for the purpose of comparison of their catalytic performance. Results of the total conversion of 1-hexene and the selectivity to aldehydes are presented. The difference between the total conversion and conversion to aldehydes corresponds to isomerisation products, mainly 2-hexene as discussed elsewhere by Chuang and Pien.[41]

The catalytic performance of RhP_2-P-Zn_3Al-LDH prepared by the new method of in situ complexation, in which free TPPTS ligands are cointercalated into LDH (P/Rh molar ratio: 7.8), is shown in Figure 5a. In the four consecutive cycles, the RhP_2-P-Zn_3Al-LDH catalyst displayed high selectivity towards aldehydes of 70–80%, low selectivity for 2-hexene of around 20–30%, and *n*/*i*-aldehyde ratios of 2.6–3.0; moreover, the activity toward aldehyde formation of RhP_2-P-Zn_3Al-LDH was rather high [Figure 5Aa, turnover frequency (TOF) = 80–150 h^{-1}]. Based on the elemental analysis data, the Rh loading for the sample of RhP_2-P-Zn_3Al-LDH after 4 cycles used is 0.44% (w/w). Compared with the Rh content before use (0.48%, Table 2), the loss of Rh in this catalyst after 4 cycles is 8.3%.

For comparative purposes, a mixture of *trans*-$RhCl(CO)(TPPTS)_2$ and TPPTS (with the same P/Rh molar ratio as that in RhP_2-P-Zn_3Al-LDH) in a water-oil biphasic catalytic system was also studied. Compared with hydroformylation over RhP_2-P-Zn_3Al-LDH, the catalyst in the water-oil biphasic catalytic system exhibited lower total conversion (10–26%). Furthermore, the value of TOF towards aldehyde of around 20–25 h^{-1} in this system was much lower than that in the RhP_2-P-Zn_3Al-LDH system, although the value of *n*/*i*-aldehyde ratio (3.5–5.7) was higher than that for RhP_2-P-Zn_3Al-LDH.

Comparison of the catalytic performance of RhP_2-P-Zn_3Al-LDH and the corresponding water-oil biphasic catalytic system reveals three main points. First, *trans*-$RhCl(CO)(TPPTS)_2$ has a much higher activity when intercalated in an LDHs than in solution. For aldehyde formation under identical reaction conditions, the value of TOF is enhanced four to six times by immobilization between the sheets of the positively charged LDH layers. The generally accepted mechanism for hydroformylation proposed by Evans et al.[42] is shown in Scheme 1. The higher activity of RhP_2-P-Zn_3Al-LDH may be ascribed to the basic nature of LDHs, which facilitates the formation of a rhodium hydride complex by removing the HCl formed (step 1 in Scheme 1A). It is also possible that the large positive electrical potential experienced by $HRh(CO)(TPPTS)_2$ in the interlayer galleries may be responsible for the superior performance. Similar observations have been reported for Heck arylation catalyzed by LDH-$Pd(TPPTS)_2$,[26] oxidative bromination catalyzed by LDH-WO_4,[18] and asymmetric dihydroxylation catalyzed by LDH-OsO_4.[43] Secondly, it can be concluded that the reusability of RhP_2-P-Zn_3Al-LDH is much better than the corresponding water-oil biphasic system. This is because of the little leaching of active species from the carrier because of the strong electrostatic interaction between the oxygen

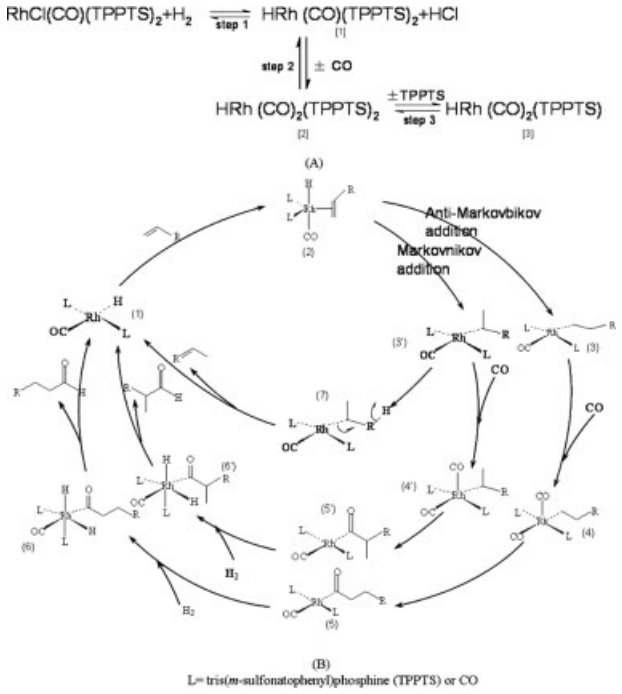

Scheme 1. Mechanism for LDHs-$HRh(CO)(TPPTS)_2$ catalyzed hydroformylation of 1-hexene.

atoms in the sulfonate groups of the interlayer *trans*-$RhCl(CO)(TPPTS)_2$ and the host lattice, which has been confirmed by FTIR spectroscopy (Figure 2f). The activity of the RhP_2-P-Zn_3Al-LDH showed a statistically significant increase on reuse, as seen in Figure 5A. It is well-known that there is an induction period during which the rhodium precursor becomes an active 16-electron complex such as $HRhCO(TPPTS)_2$ or $HRh(CO)_2$(TPPTS) under catalytic conditions,[44] as shown in Scheme 1A. It is therefore possible that the amount of active species derived from the tethered catalyst precursor increases slowly with reaction time. Finally however, it must also be noted that the value of *n*/*i* aldehyde ratio (3.5–5.7) for the water-oil biphasic system was higher than that for RhP_2-P-Zn_3Al-LDH (2.6–3.0), so that the selectivity of the water-oil biphasic system for *n*-aldehydes is better than that of RhP_2-P-Zn_3Al-LDH. This may be rationalized using the catalytic cycle (Scheme 1B), which has been taken from the literature.[42,45–47] The different ways of inserting an alkene into a metal-hydrogen bond, as shown by Route (2)→(3) and (2)→(3′), are called anti-Markovnikov and Markovnikov addition, respectively. The relative rates of these two reactions are considered to be primarily determined by the degree of steric crowding around the metal center. The normal alkyl intermediate requires less space and is therefore formed more easily than the branched one in the presence of bulky ligands. Comparing $HRhCO(TPPTS)_2$ with $HRh(CO)_2$(TPPTS), the former favors high selectivity to *n*-aldehyde. In the water-oil biphasic system, TPPTS is more mobile and may be more available for coordination to Rh compared with the RhP_2-P-Zn_3Al-LDH system, in spite of the P/Rh molar ratios being the same in the two systems. Consequently, the catalytically active species $HRhCO(TPPTS)_2$ (Scheme 1A) can form more readily than $HRh(CO)_2$(TPPTS) in the water-

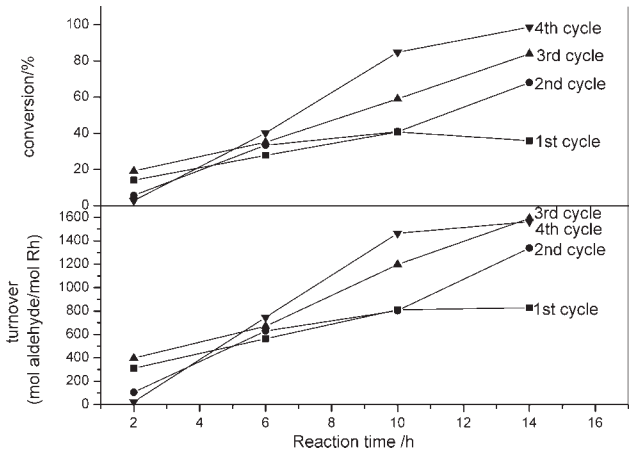

Figure 6. Conversion and turnover numbers of aldehyde formed as a function of reaction time over RhP_2-P-Zn_3Al-LDH* catalyst in 1-hexene hydroformylation.†

*Rh/1-hexene = 4.0×10^{-4}; †Reaction conditions: 1.5 ml of 1-hexene, 1.6 MPa, 100°C, $H_2/CO = 1$.

oil biphasic system, and may be responsible for the higher *n*/*i* ratios observed in this system.

As shown in Figure 5B, the sample of RhP_2-Zn_3Al-LDH prepared by the method of ion-exchange exhibited low selectivity for the hydroformylation of 1-hexene. Isomerization of C=C bonds was predominant and the value of aldehyde *n*/*i* ratio was a little lower than that for hydroformylation with the RhP_2-P-Zn_3Al-LDH catalyst. The lower amount of TPPTS in the RhP_2-Zn_3Al-LDH catalyst system compared with that in RhP_2-P-Zn_3Al-LDH should result in the formation of less $HRhCO(TPPTS)_2$ and more $HRh(CO)_2(TPPTS)$ (steps 2 and 3 in Scheme 1A), which leads to lower selectivity towards both total aldehyde and *n*-aldehyde in the RhP_2-Zn_3Al-LDH catalytic system, as discussed above. However, it can be seen from Figure 5A that the sample of ion-exchange (RhP_2-Zn_3Al-LDH) exhibited higher activity than that of RhP_2-P-Zn_3Al-LDH prepared by in situ complexation. The main reason is that the Rh loading in the former sample is much higher than that of in the latter (3.44 and 0.48%, respectively, Table 2).

To study the influence of reaction time on the performance if the RhP_2-P-Zn_3Al-LDH catalyst in hydroformylation of 1-hexene, the results at the end of four consecutive 2, 6, 10, and 14-h cycles are compared in Figure 6. The system maintained hydroformylation activity throughout the 14-h reaction time, as turnover of aldehyde increased continuously. It can also be seen that the turnover of aldehyde for the third and fourth cycles increased faster with reaction time than that in the first two cycles. This indicates that the RhP_2-P-Zn_3Al-LDH catalyst can maintain its activity unchanged during prolonged hydroformylation times. The experimental results confirm the high stability of the intercalated rhodium complex and its ability to be effectively reused.

The Zn/Al molar ratio in RhP_2-P-Zn_nAl-LDH was also varied and the catalytic behavior of the resulting composites was studied (Figure 7). It is well known that electrostatic forces give rise to strong interactions between the interlayer anions and the LDH host lattice. With the increase in Zn/Al molar ratio of the host layers, the electron density of the host lattices decreases and thus leads to a decrease in the concentration of guest anions in the interlayer galleries. This is confirmed by comparison of RhP_2-P-Zn_2Al-LDH and RhP_2-P-Zn_3Al-LDH, whose rhodium loadings are 0.90 and 0.48%, respectively. As a result, the activity of the former is higher than that of the latter, represented by the sharp decrease in the conversion from 81 to 28% (as shown in Figure 7) as the Zn/Al ratio increases from 1.9 to 2.6. However, as the Zn/Al ratio increased from 2.6 to 3.9, the content of Rh increased slightly (from 0.48 to 0.60%), and the conversion increased from 28 to 35%. The slight increase in rhodium loading may result from the low crystallinity of RhP_2-P-Zn_4Al-LDH [as shown by the XRD pattern (Figure 1f)], which favors the adsorption of some rhodium complex on the surface of the LDH.

As far as catalytic selectivity is concerned, it was found that the selectivity towards both total aldehyde and *n*-aldehyde increased with increasing Zn/Al ratio of the samples (Figure 7). This phenomenon can be explained as follows: the lower the Zn/Al ratio, the higher the electron density of the host layers, the higher the concentration of interlayer anions, and thus the more severe the steric crowding. This leads to fewer free ligands (TPPTS) being available near the active species ($HRhCO(TPPTS)_2$). On increasing the Zn/Al ratio, the content of the interlayer catalytic species decreases and the steric crowding becomes less significant, and as a result, more of the TPPTS ligands may be able to coordinate to the rhodium centers. According to the catalytic mechanism (Scheme 1A), the catalytically active species $HRhCO(TPPTS)_2$ (Scheme 1A1) is favored over $HRh(CO)_2(TPPTS)$ (Scheme 1A3) in the presence of large concentration of free ligands, and the former species with its sterically crowded environment around the metal center favors anti-Markovni-

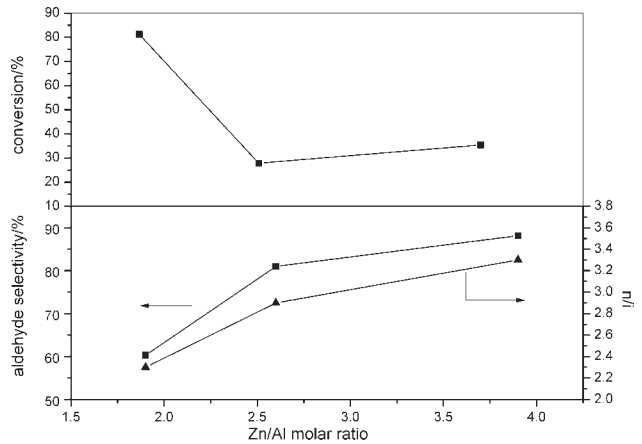

Figure 7. Conversion and selectivity as a function of Zn/Al molar ratio of LDHs over RhP_2-P-Zn_nAl-LDH* catalyst in 1-hexene hydroformylation.†

*Rh/1-hexene = 4.0×10^{-4}, $n = 2$, 3, and 4; †Reaction conditions: 1.5 ml of 1-hexene, 1.6 MPa, 100°C, $H_2/CO = 1$, 6-h reaction time.

kov addition. This leads to the observed increase in selectivity towards *n*-aldehyde on increasing the Zn/Al ratio.

Conclusions

Cointercalation of the Rh-complex *trans*-RhCl(CO)$(TPPTS)_2$ and the ligand TPPTS into inorganic LDH hosts was successfully accomplished by the method of in situ complexation, and the catalytic performance of the resulting material in the hydroformylation of alkenes has been investigated. It was found that the new catalyst showed higher activity towards aldehyde formation and better reusability compared with the corresponding water-oil biphasic catalytic system under similar reaction conditions. It is suggested that the basic nature of the support, the large positive electrical potential of the host LDHs, and the spatial orientation of the intercalated guests (*trans*-RhCl(CO)$(TPPTS)_2$ as well as TPPTS) are responsible for the superior catalytic performance. Strong interactions occur between the LDH layers and the active rhodium species on intercalation, resulting in the good reusability. Furthermore, the catalyst prepared by the method of in situ complexation (RhP_2-P-Zn_nAl-LDH) showed much higher catalytic activity and selectivity towards aldehydes compared with that of an intercalated complex prepared by ion exchange. It was found that increasing the Zn/Al molar ratio in RhP_2-P-Zn_nAl-LDH led to lower activity and higher selectivity to both total aldehyde and *n*-aldehyde, which can be related to the content of Rh and the availability of the free ligand, respectively.

Acknowledgments

This project was supported by the National Natural Science Foundation Major International Joint Research Program (Grant No. 20620130108), National Natural Science Foundation of China (Grant No. 20601001), the Program for New Century Excellent Talents in University (Grant No. NCET-05-121), the 111 Project (Grant No. B07004) the Program for Changjiang Scholars and Innovative Research Team in University (PCSIRT) and National Natural Science Foundation Key Project of China (Grant No. 90306012).

Literature Cited

1. Dickson RS. Homogeneous Catalysis with Compounds of Rhodium and Iridium. New York: Springer, 1985.
2. Cornils B. *New Synthesis with Carbon Monoxide*. New York: Springer, 1980.
3. Hartley FR. *Supported Metal Complexes*. Dordrecht: Reidel, 1985.
4. Hung KGW, Papadias D, Björnbom P, Anderlund M, Åkermark B. Reverse-flow operation for application of imperfectly immobilized catalysts. *AIChE J*. 2003;49:151–167.
5. Lenarda M, Storaro L, Ganzerla R. Hydroformylation of simple olefins catalyzed by metals and clusters supported on unfunctionalized inorganic carriers. *J Mol Catal A*. 1996;111:203–237.
6. Huang L, Kawi S. An active and stable Wilkinson's complex-derived SiO_2-tethered catalyst via an amine ligand for cyclohexene hydroformylation. *Catal Lett*. 2004;92:57–62.
7. Dossi C, Fusi A, Garlaschelli L, Psaro R, Ugo R. *Proceedings of the 10th International Congress on Catalysis*, Budapest, 1992.
8. Ichikawa M. Catalytic hydroformylation of olefins over the rhodium, bimetallic Rh-Co, and cobalt carbonyl clusters supported with some metal oxides. *J Catal*. 1979;59:67–78.
9. Mukhopadhyay K, Mandale AB, Chaudhari, RV. Encapsulated $HRh(CO)(PPh_3)_3$ in microporous and mesoporous supports: novel heterogeneous catalysts for hydroformylation. *Chem Mater*. 2003;15:1766–1777.
10. De Vos DE, Thibault-Starzyk F, Knops-Gerrits PP, Parton RF, Jacobs PA. A critical overview of the catalytic potential of zeolite supported metal complexes. *Macromol Symp*. 1994;80:157–184.
11. Wulf G. Molecular imprinting in cross-linked materials with the aid of molecular templates—a way towards artificial antibodies. *Angew Chem Int Ed*. 1995;34:1812–1832.
12. Müller A, Reuter H, Dillinger S. Supramolecular inorganic chemistry: small guests in small and large hosts. *Angew Chem Int Ed*. 1995;34:2328–2361.
13. Cavani F, Trifirò F, Vaccari A. Hydrotalcite-type anionic clays: preparation, properties and application. *Catal Today*. 1991;11:173–301.
14. Khan AI, O'Hare D. Intercalation chemistry of layered double hydroxides: recent developments and applications. *J Mater Chem*. 2002;12:3191–3198.
15. Meyn M, Beneke K, Lagaly G. Anion-exchange reactions of layered double hydroxides. *Inorg Chem*. 1990;29:5201–5207.
16. Newman SP, Jones W. *Supramolecular Organization and Materials Design*. Cambridge: Cambridge University Press, 2001.
17. Ogawa M, Kuroda K. Photofunctions of intercalation compounds. *Chem Rev*. 1995;95:399–438.
18. Sels B, Vos DD, Buntinx M, Pierard F, Mesmaeker AKD, Jacobs P. Layered double hydroxides exchanged with tungstate as biomimetic catalysts for mild oxidative bromination. *Nature*. 1999;400:855–857.
19. Lei XD, Zhang FZ, Yang L, Guo XX, Tian YY, Fu SS, Li F, Evans DG, Duan X. Highly crystalline activated layered double hydroxides as solid acid-base catalysts. *AIChE J*. 2007;53:932–940.
20. Newman SP, Jones W. Synthesis, characterization and applications of layered double hydroxides containing organic guests. *New J Chem*. 1998;22:105–115.
21. Corma A, Fornes V, Rey F, Cervilla A, Llopis E, Ribera A. Catalytic air oxidation of thiols mediated at a $Mo(VI)O_2$ complex center intercalated in a Zn(II)-Al(III) layered double hydroxide host. *J Catal*. 1995;152:237–242.
22. Pinnavaia TJ, Chibwe M, Constantino VRL, Yun SK. Organic chemical conversions catalyzed by intercalated layered double hydroxides (LDHs). *Appl Clay Sci*. 1995;10:117–129.
23. Bhattacharjee S, Anderson JA. Synthesis and characterization of novel chiral sulfonato–salen–manganese(iii) complex in a zinc–aluminium LDH host. *Chem Commun*. 2004;4:554–555.
24. Choudary BM, Madhi S, Chowdari NS, Kantam ML, Sreedhar B. Layered double hydroxide supported nanopalladium catalyst for Heck-, Suzuki-, Sonogashira-, and Stille-type coupling reactions of chloroarenes. *J Am Chem Soc*. 2002;124:14127–14136.
25. Zhang X, Wei M, Pu M, Li XJ, Chen H, Evans DG, Duan X. Preparation and characterization of trans-RhCl(CO)$(TPPTS)_2$-intercalated layered double hydroxides. *J Solid State Chem*. 2005;178:2701–2707.
26. Choudary BM, Kantam ML, Reddy NM, Gupta NM. Layered-double-hydroxide- supported $Pd(TPPTS)_2Cl_2$: a new heterogeneous catalyst for Heck arylation of olefins. *Catal Lett*. 2002;82:79–83.
27. Kuntz EG. Catalytic hydroformylation of olefins. US Patent 4,248,802, 1981.
28. Li XJ, Chen H, Li YZ, Liu HC. Preparation of RhCl(CO)$(TPPTS)_2$ (TPPTS: trisodium salt of tri-(m-sulfophenyl)-phosphine), Chinese Patent 1,179,429, 1998.
29. Drezdon MA. Pillared hydrotalcites. US Patent 4,774,212, 1988.
30. Bookin AS, Drits V. Polytype diversity of the hydrotalcite-like minerals I. Possible polytypes and their diffraction features. *Clays Clay Miner*. 1993;41:551–557.
31. Vaysse C, Guerlou-Demourgues L, Delmas C. Thermal evolution of carbonate pillared layered hydroxides with (Ni, L) (L = Fe, Co) based slabs: grafting or nongrafting of carbonate anions. *Inorg Chem*. 2002;41:6905–6913.
32. Bonnet S, Forano C, de Roy A, Besse JP, Maillard P, Momenteau M. Synthesis of hybrid organo-mineral materials: anionic tetraphenylporphyrins in layered double hydroxides. *Chem Mater*. 1996;8:1962–1968.
33. Xu ZP, Zeng HC. Abrupt structural transformation in hydrotalcite-like compounds $Mg_{1-x}Al_x(OH)_2(NO_3)_x{\cdot}nH_2O$ as a continuous function of nitrate anions. *J Phys Chem B*. 2001;105:1743–1749.
34. Herrmann WA, Kellner J, Riepl H. Wasserlösliche Metallkomplexe und Katalysatoren III. Neue wasserlösliche Metallkomplexe des sulfonierten Triphenylphosphans (TPPTS): Mn, Fe, Ru, Co, Rh, Ir, Ni, Pd, Pt, Ag, Au. *J Organomet Chem*. 1990;389:103–128.

35. Li F, Zhang LH, Evans DG, Forano C, Duan X. Structure and thermal evolution of Mg–Al layered double hydroxide containing interlayer organic glyphosate anions. *Thermochim Acta*. 2004;424:15–23.
36. Nakanishi K. *IR Absorption Spectroscopy-Practical*. Tokyo: Nankodo, 1960.
37. Kanezaki E. Intercalation of naphthalene-2,6-disulfonate between layers of Mg and Al double hydroxide: preparation, powder X-ray diffraction, fourier transform infrared spectra and X-ray photoelectron spectra. *Mater Res Bull*. 1999;34:1435–1440.
38. Kanezaki E. Fourier transform infrared spectra of naphthalene disulfonates between layers of Mg and Al double hydroxide: intercalation by means of coprecipitation and direct observation of coordination from the interlayer anion to the metal cation in the layer. *J Incl Phenom Macrocyclic Chem*. 2000;36:447–453.
39. Kanezaki E. Unexchangeable interlayer anions; synthesis and characterization of Zn/Al- and Mg/Al-layered double hydroxides with interlayer alizarin red S. *J Incl Phenom Macrocyclic Chem*. 2003;46:89–95.
40. Herrmann WA, Kulpe JA, Kellner J, Riepl H, Bahrmann H, Konkel W. Water-soluble metal complexes of the sulfonated triphenylphosphine. *Angew Chem Int Ed Engl*. 1990;29:391–393.
41. Chuang SSC, Pien SI. Infrared study of the CO insertion reaction on reduced, oxidized, and sulfided Rh/SiO_2 catalysts. *J Catal*. 1992;135:618–634.
42. Evans D, Osborn JA, Wilkinson G. Hydroformylation of alkenes by use of rhodium complex catalysis. *J Chem Soc A*. 1968;12:3133–3142.
43. Choudary BM, Chowdari NS, Kantam ML, Raghavan KV. Catalytic asymmetric dihydroxylation of olefins with new catalysts: the first example of heterogenization of OsO_4^{2-} by ion-exchange technique. *J Am Chem Soc*. 2001;123:9220–9221.
44. Huang L, Kawi S. An active and stable Wilkinson's complex-derived SiO_2-tethered catalyst via an amine ligand for cyclohexene hydroformylation. *Catal Lett*. 2004;92:57–62.
45. Brown CK, Wilkinson G. Homogeneous hydroformylation of alkenes with hydridocarbonyltris -(triphenylphosphine)rhodium(i) as catalyst. *J Chem Soc A*. 1970;14:2753–2762.
46. Yang C, Mao Z, Wang Y, Chen J. Kinetics of hydroformylation of propylene using $RhCl(CO)(TPPTS)_2$/TPPTS complex catalyst in aqueous system. *Catal Today*. 2002;74:111–119.
47. Bhaduri S, Mukesh D. *Homogeneous Catalysis: Mechanism and Industrial Applications*. New York: Wiley, 2000.
48. Herrmann WA, Kulpe JA, Konkol W, Bahrmann H. Wasserlösliche Metallkomplexe und Katalysatoren II. Verfahren zur Reindarstellung von Tris(natrium-*m*-sulfonatophenyl)phosphan (TPPTS) und katalyserelevanter Rhodium-Komplexe. *J Organomet Chem* 1990;389:85–101.

Manuscript received May 5, 2007, and revision received Aug. 21, 2007.